Supporting Information

Bristow et al. 10.1073/pnas.1616649114

SI Text

Model Details. The reaction–transport model was developed in R—an open source statistical computing environment (38). ReacTran, a package of functions, routines, and solvers for reactive–transport modeling, was used (39). In addition, functions in packages seacarb and marelec are used to calculate initial carbonate speciation in the water column based on specified P_{CO2} and pH, as well as equilibrium constants and diffusion coefficients of chemical species under the specified physical and chemical conditions (40, 41).

The model finds a numerical solution to a set of three ordinary differential equations describing the temporal change in total dissolved inorganic carbon (DIC), pH, and siderite concentration in a one-dimensional porous sedimentary profile subject to diffusion and advection (transport) associated with sedimentary accumulation, and chemical reactions. The model equations were formulated using the direct substitution approach (42). Tracking temporal changes in the pH and DIC of the model domain allows calculation of the concentration of any species of inorganic carbon (e.g., ref. 43).

Exchange with lake water, assumed to behave as an infinite reservoir and represented by the upper boundary condition imposed on the model domain, occurs by diffusion only. As described in the main text and shown in Figs. 2 and 3, simulations are run with a range of lake water chemistries constrained to be in equilibrium with prescribed atmospheric CO_2 levels and lake water pH.

The rate of siderite precipitation follows the general scheme described in the main text and depends on the saturation state of pore waters with respect to siderite (Ω), given by

$$\Omega_{FeCO_3} = \frac{[Fe^{2+}]\,[CO_3^{2-}]}{K_{sp}}, \qquad \text{[S1]}$$

where K_{sp} is the solubility product of siderite calculated with the formulation of ref. 44 and adjusted with salinity following ref. 45.

$[CO_3^{2-}]$ is calculated at each time step from DIC and pH. As justified in the main text, $[Fe^{2+}]$ is set to be saturated with respect to either magnetite or fayalite as represented by reactions S2–S4. In the case of reaction S2 O_2(aq) activity is set to equal the magnetite/hematite boundary.

$$\text{Magnetite} + 2[H^+] = [Fe^{2+}] + [H_2O] + \text{Hematite}, \qquad \text{[S2]}$$

$$\text{Fayalite} + 4[H^+] = 2[Fe^{2+}] + \text{Quartz} + 2[H_2O], \qquad \text{[S3]}$$

or

$$\text{Fayalite} + 4[H^+] = 2[Fe^{2+}] + \text{Amorphous silica} + 2[H_2O]. \qquad \text{[S4]}$$

SUPCRT, implemented in the R package CHNOSZ (46), was used to calculate equilibrium constant of these reactions at given temperature and salinity values. $[Fe^{2+}]$ is calculated within the model profile at each time step based on pH and provides a lower limit on $[Fe^{2+}]$.

Ω_{FeCO3} is linked to carbonate precipitation rates by the expression:

$$R_{sidprec} = k_{sidprec}(\Omega_{FeCO_3} - 1)^n. \qquad \text{[S5]}$$

Here, $k_{sidprec}$ is the kinetic constant for siderite precipitation and n is the order of the reaction. We use the lowest value of $k_{sidprec}$ (0.05 mmol·kg^{-1}·y^{-1} at 25 °C) available from the literature (Table S1) because the aim is to obtain an upper bound on atmospheric P_{CO2}. $k_{sidprec}$ varies with temperature ($k_{sidprecT}$) according to

$$K_{sidprecT} = K_{sidprec25} \cdot e^{\frac{-Ea}{R}\left(\frac{1}{T} - \frac{1}{298.15\ \text{K}}\right)}. \qquad \text{[S6]}$$

An activation energy (Ea) of 54 kJ/mol was used based on the experimental work of Johnson (50). Siderite precipitation shows a first-order dependence on saturation state thus $n = 1$ (48).

Simulations are initiated with DIC, pH, and siderite content set to zero throughout the model sediment column. When the model is run, siderite precipitates and is buried, a process that consumes DIC. The depth of the model domain is manually adjusted through trial and error to ensure negligible carbonate is being added at the base of the model profile. Model profiles are typically ∼1.5 m deep and split into 45 layers. Model results are collected after equilibrium is assured, an interval of 250 y. Typical equilibrium outputs of a model run are shown in Fig. S4.

Comparison of Olivine Dissolution and Siderite Precipitation Kinetics. As discussed in the main text, the model formulation implemented assumes that siderite precipitation kinetics limit carbonate production rather than Fe^{2+} supplied by the dissolution of olivine. Fig. S3 compares olivine dissolution rates from pH 5–10 with siderite precipitation rates for a range of siderite saturation states observed in model simulations (Ω). Olivine dissolution rate calculations follow the formulation of ref. 51 and a specific surface area of 5 m^2/g, measured on olivine powder with similar grain size as the Sheepbed mudstone at YKB (52). Olivine dissolution always outpaces siderite precipitation.

Sensitivity Tests. Fig. 2 shows results of model sensitivity analysis of P_{CO2} thresholds to sedimentary porosity, temperature, and salinity, respectively.

Sedimentary porosity. Terrestrial muds deposits that have not been buried typically have porosities of 0.6–0.8 (31). Fig. 2*A* shows the influence on P_{CO2} thresholds of increasing sedimentary porosity values up to 0.8, from the value of 0.6 used in model runs discussed in the main text. The result is a ∼threefold decrease in P_{CO2} threshold, regardless of burial rate. This confirms that using a porosity value of 0.6 provides an upper threshold on P_{CO2}.

Temperature. Fig. 2*B* shows that as temperature increases the upper threshold on P_{CO2} also increases. However, the increase is insignificant (∼10s mbar in the model scenario with a sedimentary porosity of 0.6 and burial rate of 1 cm/y), compared with the amounts of CO_2 needed in climate models to push martian climate to these higher temperatures.

Salinity. P_{CO2} thresholds are higher when water is either fresh or saline (Fig. 2*B*). In the model scenario presented in Fig. 2*B*, P_{CO2} thresholds vary by as much as ∼30 mbar at 5 °C with the highest thresholds (100 mbar) obtained when waters are fresh. As discussed in the text, salinity appears to have been low at the time of deposition of YKB sediments, based on limited Cl and S concentration in the sedimentary matrix and the lack of detection of evaporative minerals in the mudstone (12). Uncertainty in the exact salinity of pore waters does not impact the conclusions drawn from our work.

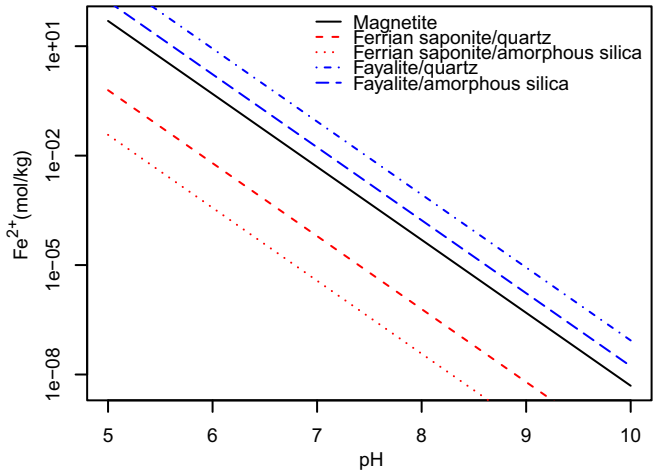

Fig. S1. Thermodynamic stability diagram showing the Fe^{2+} concentration required to be in equilibrium with various minerals and silica activities ranging from quartz to amorphous silica, as a function of pH. Lines show saturation values at 10 °C and a salinity of 10 g/kg. Minerals are supersaturated above their respective equilibrium lines. All thermodynamic data come from ref. 53 with the exception of Fe saponite ($Na_{0.35}Fe_3Al_{0.35}Si_{3.65}O_{10}OH_2$) determined in ref. 16. In drawing the stability boundaries for magnetite, redox state is set at the magnetite/hematite boundary, as detailed in the main text. In defining equilibrium lines for ferrian saponite, Al^{3+} is set to saturation with respect to albite, which is reasonable given that the Sheepbed contains ∼20 wt % plagioclase feldspar (9).

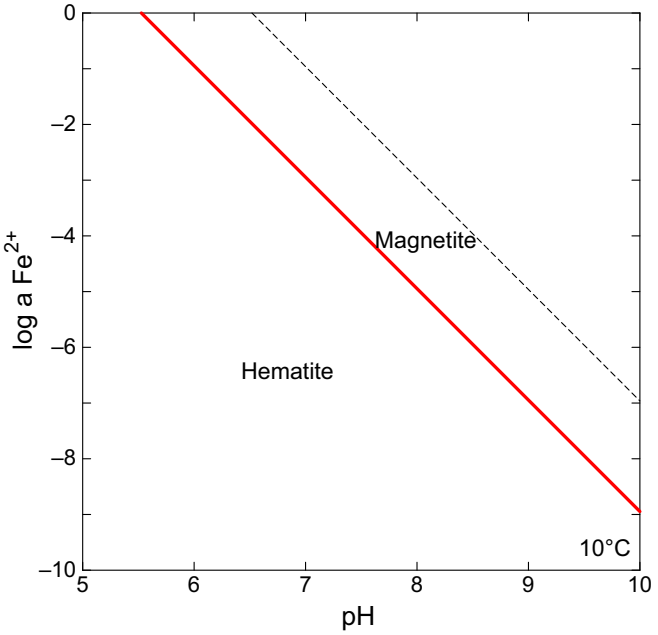

Fig. S2. Thermodynamic stability diagram showing the relation between Fe^{2+} activity (red line) and pH with redox state at the magnetite/hematite boundary. Note that in more oxidizing conditions magnetite is unstable. Under more reducing conditions Fe^{2+} activity is higher and thus the resulting P_{CO2} threshold estimated using the reaction–transport model is reduced. The figure was generated using Geochemist's Workbench for illustrative purposes. In the model [Fe^{2+}] was calculated at a given pH, temperature and salinity using SUPCRT, as described in *SI Text, Model Details*.

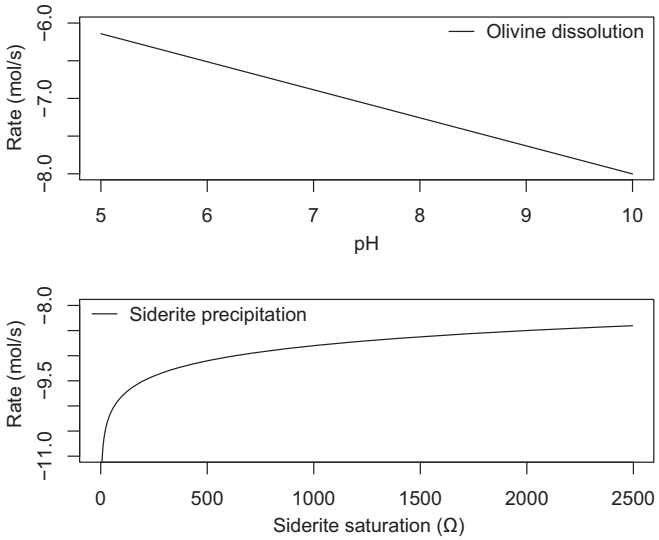

Fig. S3. Comparison of olivine dissolution rates over a range of pH values with siderite precipitation rates at various values of Ω. *SI Text, Comparison of Olivine Dissolution and Siderite Precipitation Kinetics* describes details of how rates were derived.

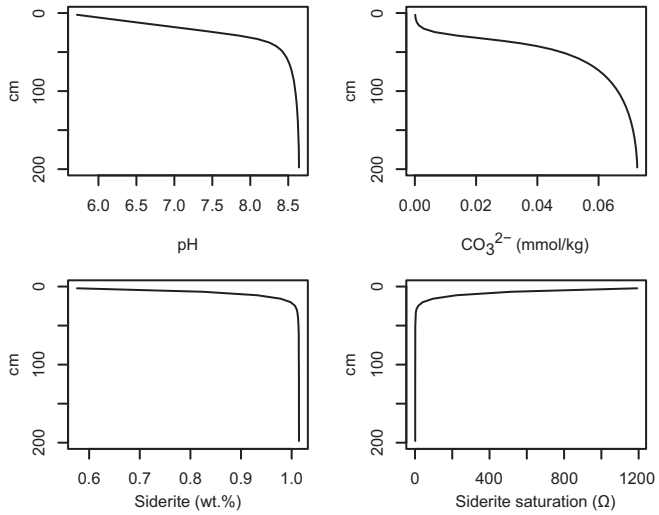

Fig. S4. Typical reaction–transport model output. The four panels show calculated changes in pH, DIC, siderite content and saturation with respect to siderite with depth below sediment/water interface. In this simulation, porosity within the model profile is 0.6, sediment accumulation rate is 1 cm/y, temperature is 10 °C and salinity is 10 g/kg. Carbonate speciation and concentrations at the upper model boundary, representing lake waters, are set to be in equilibrium at pH 5.5 with an atmospheric P_{CO2} of 63 mbars.

Table S1. Rate constants for siderite precipitation

Rate constant (mmol·kg^{-1}·y^{-1})	Refs.
0.050	47
0.053	48
12.623	49